

Autoradiography and Radioscintigraphy of Technetium-99m-Sestamibi in c-neu Transgenic Mice

Paul D. Crane, David C. Onthank, Cheryl R. Bourque, Stuart J. Heminway, Theresa J. Mazaika, Irwin Leav, Grace F. Zambuto, Joel L. Lazewatsky, Laura Villamil-Perez and Timothy R. Carroll

Radiopharmaceutical Division, DuPont Merck Pharmaceutical Co., North Billerica, Massachusetts; and Department of Pathology, Tufts University School of Veterinary Medicine, Boston, Massachusetts

Intratumor distribution patterns of ^{99m}Tc -sestamibi and ^{14}C -2-deoxy-D-glucose were compared in the c-neu OncoMouse™, a transgenic mouse that spontaneously develops breast tumors. **Methods:** Thirty or 60 min after intravenous injection of 5 μCi ^{14}C -2-deoxy-D-glucose and 3 mCi ^{99m}Tc -sestamibi into mice ($n = 3$ per time point) bearing mammary tumors (0.3–1.5 cm), the animals were analyzed for organ and tumor distribution using dual-label, whole-body autoradiography. The retention patterns of the two compounds were related to tumor morphology and viability, based on H&E-stained adjacent sections. For imaging studies, the transgenic mice ($n = 9$) were anesthetized with pentobarbital, injected intravenously with 5–20 mCi ^{99m}Tc -sestamibi and imaged for 60 min using a gamma camera equipped with a 1-mm pinhole collimator. **Results:** All positively stained tumors retained both agents, with a mean ^{99m}Tc -sestamibi tumor retention of $0.38\% \pm 0.2\%$ ID/g at 30 min compared to $4.18\% \pm 0.62\%$ ID/g for ^{14}C -2-deoxy-D-glucose. Tumor retention of the agents remained the same at 60 min, and neither compound localized within necrotic or cystic regions of the neoplasms. Repeat imaging at 2–8-day intervals indicated a predicted sensitivity to detect a 30% difference in tumor retention of a test versus reference compound in preclinical screening. **Conclusion:** The c-neu OncoMouse™ is a useful model for in vivo imaging and provides a spontaneous tumor model for preclinical screening of breast tumor imaging agents.

Key Words: breast tumor; technetium-99m-sestamibi; carbon-14 deoxyglucose; transgenic mouse

J Nucl Med 1995; 36:1862–1868

Radiopharmaceuticals can play an important role in tumor imaging, both by retention based on functional differences between normal and tumor tissue, as well as by distinguishing viable from necrotic tissue. This strategy has been successfully used in several agents to image human breast cancers. PET with ^{18}F -2-fluoro-2-deoxy-D-glucose,

a glucose analog, has been used to detect neoplasms by their elevated glycolytic activity (1,2). Indium-111-DTPA-pentetretotide localizes within breast carcinoma by binding to somatostatin receptors (3). Thallium-201, which is taken up into cells by the Na, K ATPase transport pump (4), can distinguish malignant from benign breast lesions (5,6).

Recently, ^{99m}Tc -sestamibi retention in human breast tumors has been examined [for review, see Khalkhali et al. (7)]. Technetium-99m-sestamibi is known to be retained within the heart in direct proportion to blood flow (8). Although the tumor retention mechanism is not fully understood in all organs tested, the agent is retained within the mitochondria (9) by a mechanism dependent on the maintenance of membrane potential within this organelle (10).

The development of improved tumor imaging agents requires preclinical optimization screening that examines tumor targeting (or tumor vasculature) as well as discriminating viability from necrosis. This is commonly accomplished with xenograft nude rodent models, which permit a large variety of implanted tumor types for analysis (11). Disadvantages of the model, however, include abnormally positioned tumors, a tumor circulatory bed developing post-implantation and a resulting differentiation and tumor architecture often different from that found in spontaneous cancers. Thus, xenograft model systems do not accurately replicate the situation found in spontaneous cancers, and their use may confound efforts at optimizing receptor binding, vascular permeability or metabolic interaction.

This study assesses the c-neu OncoMouse™ as an alternative in vivo screening model for a breast tumor imaging agent. This transgenic mouse has a predisposition for developing breast neoplasms that arise in conjunction with angiogenic processes that closely parallel spontaneous tumor growth (12,13). Our study compares the regional retention of ^{99m}Tc -sestamibi in the c-neu OncoMouse™ with ^{14}C -2-deoxy-2-D-glucose ($[^{14}\text{C}]2\text{DG}$). Using whole-body autoradiography, which combines the localization of radio-substrate with histological evaluation, the distribution of the two agents was found to be directly related to tissue viability and the growth pattern of the neoplasm. To deter-

Received Dec. 15, 1994; revision accepted May 25, 1995.

For correspondence or reprints contact: Paul D. Crane, PhD, Radiopharmaceutical Division, Du Pont Merck Pharmaceutical Co., 331 Treble Cove Rd., N. Billerica, MA 01862.

mine the relative availability of the imaging agents to the tumors from the circulation, blood clearance curves were also obtained for ^{99m}Tc -sestamibi, [^{14}C]2DG and ^{201}Tl . A planar imaging protocol is also presented as an *in vivo* preclinical screening test.

MATERIALS AND METHODS

Experimental Design

The specificity of ^{99m}Tc -sestamibi retention in spontaneous breast tumors was examined using dual-label whole-body autoradiography. Organ and tumor distribution was compared to that of [^{14}C]2DG, a positive control, using microdensitometry of registered ^{14}C and ^{99m}Tc images. The animals were examined at 30 or 60 min after intravenous administration of the compounds ($n = 3$ per time point). The distribution patterns of the two compounds were directly compared with tissue viability as determined by histological examination. The purpose of these studies was to relate the pattern of ^{99m}Tc -sestamibi tumor retention to that of the tumor structure. The blood activity of ^{99m}Tc -sestamibi and [^{14}C]2DG was also assessed over a 60-min time course in comparison with ^{201}Tl . Thallium-201 was included as another agent with known affinity for human breast tumors (6).

The utility of the OncoMouse™ model as a preclinical screening test for breast tumor imaging agents was investigated using a gamma camera equipped with a pinhole collimator. The background pattern of ^{99m}Tc -sestamibi was determined using the FVB wild type mouse, from which the c-neu transgenic mouse was derived. Tumor retention was determined from regions of interest (ROIs) after correction for administered dose. The between-day variance of intratumor retention was estimated using crossover protocol.

Radioisotopes

Thallium-201 was obtained from DuPont Pharma (N. Billerica, MA). The preparation of ^{99m}Tc -sestamibi and quality control for radiochemical purity was done following the manufacturer's instructions. Carbon-14-2-deoxy-D-glucose (uniform label; specific activity, 300–350 mCi/mmol) in sterile water was obtained from DuPont NEN Research Products (Boston, MA).

Animals

FVB mice and female c-neu transgenic mice were obtained from Charles River Labs (Boston, MA) and DuPont NEN, respectively. The presence of the c-neu transgene was verified by polymerase chain reaction assay. Tumor-bearing mice, 23–40 g, were selected for use when palpable breast tumors (0.3–1.5 cm diameter) appeared. FVB mice, 19–30 g, were used as nontumor controls.

Blood Kinetics

Tumor-bearing mice were injected intravenously (tail vein) with a 0.2-ml bolus containing 2 mCi ^{99m}Tc -sestamibi, 0.3 mCi ^{201}Tl and 5 μCi [^{14}C]2DG. At 5, 15 and 60 min postinjection, the mice were anesthetized with ether and a 0.1-ml retro-orbital blood specimen was taken. At 60 min, the mice were killed by cervical dislocation. Blood samples (0.01–0.05 g) were weighed and assayed in a gamma counter for ^{99m}Tc and ^{201}Tl activity. The specimens were then digested with 1 ml Protosol® (DuPont NEN) isopropanol 1:1 (v/v) at 60°C, decolorized after cooling with 0.5 ml 30% H_2O_2 and mixed with 10 ml acidified (0.05 ml 0.5N HCl/mL) Aquasol® (Packard, Meriden, CT) scintillation fluid. The samples were stored for 30 days to permit ^{201}Tl decay and then assayed for

^{14}C activity in a liquid scintillation spectrometer. Activities were corrected for decay and expressed as the percent injected dose per gram (% ID/g).

Whole-body Autoradiography and Histology

The transgenic mice were injected intravenously (tail vein) with a 0.1-ml bolus containing 3 mCi ^{99m}Tc -sestamibi and 5 μCi [^{14}C]2DG. At either 30 or 60 min postinjection, the mice were killed by CO_2 inhalation. The entire animal was then immersed in embedding media (Histoprep, Fisher Scientific) and frozen in a 2-methyl butane/dry ice bath. The embedded bodies were then mounted onto 50 × 70 mm² prechilled stainless steel blocks and serially sectioned in a cryomicrotome (Hacker Inst., Fairfield, NJ) at -20°C . At depths of interest selected to obtain all desired organs, three consecutive sagittal whole-body 20-micron sections were taken as well as three replicate 5-micron slices for histological studies. The histological specimens were stained with hematoxylin and eosin (H&E) and photomicrographs were taken of the areas of interest. The 20-micron sections were lifted with double-sided tape and mounted onto cardboard along with ^{14}C standards (1.1–35 $\mu\text{Ci/g}$, Amersham).

A cross-calibration procedure was used to calculate ^{99m}Tc $\mu\text{Ci/g}$ values from ^{99m}Tc autoradiograms, using ^{14}C commercial standards (14). The paste preparation was a modification of Ito and Brill (15). A chicken liver paste homogenate was prepared in 10 volumes of 0.9% NaCl and centrifuged at 10,000 × g for 10 min. The supernatant was discarded and the pellet mixed with a minimal volume of 0.9% NaCl to produce a paste. Approximately 1 ml of the paste was transferred to each of six tubes containing 0.1 ml of 0.9% NaCl and serial dilutions of a known concentration of [^{99m}Tc]-pertechnetate. Technetium-99m liver paste standards were prepared by mixing the paste with the [^{99m}Tc]-pertechnetate solutions and vortexing 5 times for 10–15 sec each. Duplicate samples of each ^{99m}Tc paste suspension were transferred to pre-weighed scintillation vials, and ^{99m}Tc activity per gram of liver paste was determined by weighing and subsequent counting of activity in a gamma counter. The ^{99m}Tc paste preparations were packed into plastic straws, frozen on dry ice, and 20-micron sections of each standard paste were obtained in a cryomicrotome.

The mounted sections and standards were placed in an x-ray cassette with SB5 x-ray film (Kodak, Rochester, NY) for 3 hr at -20°C and the film was developed to obtain ^{99m}Tc images. The mounted specimens were stored for 5 days at -20°C to allow the ^{99m}Tc to decay. The specimens were then repacked with fresh film at -20°C for 5 days to obtain ^{14}C images. The optical density produced by ^{14}C and ^{99m}Tc on the films was determined using a video-based computerized microdensitometry system (LOATS, Westminster, MD) and converted to microcuries per gram based on their assigned values. A calibration equation was derived from three ^{99m}Tc liver paste studies, relating the optical density produced by ^{14}C -methylmethacrylate strips to that of the ^{99m}Tc liver paste standards:

$$y = 0.41x + .01 \quad (r^2 = 0.92, p = .0001, \text{ s.e.e.} = 0.36),$$

where $y = ^{14}\text{C}$ activity and $x = ^{99m}\text{Tc}$ activity. The ^{99m}Tc activity in animal sections was subsequently obtained by solving for x in this equation, and based on the ^{14}C -methylmethacrylate standards. Technetium-99m and ^{14}C images of each section were registered for quantitation. ROIs were sampled from the registered images and activities were expressed as percent injected dose per gram. Intratumor distribution of ^{99m}Tc and ^{14}C was

compared by line segment analysis and expressed as percent of optical density normalized to the maximum value.

Imaging

The mouse was anesthetized intraperitoneally with sodium pentobarbital (80 mg/kg) and positioned supine on a surgical board. Tumors were measured with dial calipers, and tumor size and position were recorded on mouse templates. A 0.1–0.2-ml bolus injection containing 5–20 mCi ^{99m}Tc -sestamibi in 0.15 ml saline was administered intravenously (tail vein) and the animal was placed under a gamma camera, 3 cm from a 1-mm pinhole collimator. Six 10-min images were acquired from 10 to 70 min after injection using an acquisition matrix of 256×256 pixels. A subsequent 10-min whole-body image was acquired 15 cm from the collimator to determine whole-body activity, including the tail.

The animals were allowed to recover, and the procedure was repeated 2–8 days later to determine intratumor between-day variability of ^{99m}Tc -sestamibi retention. This magnitude of variance determines the sensitivity of the method to detect differences between test and reference compounds in a preclinical screening test. Total injected activity was calculated by measuring the syringe activity before and after injection and correcting for decay. ROIs were taken, and the image data were normalized for injected dose.

Statistics

Results are expressed as the mean \pm s.d. Three types of analyses were performed $p < 0.05$ as statistically significant:

1. Autoradiography: Differences in tissue retention over time were analyzed independently by tissue type using the Student's *t*-test.
2. Blood clearance: Differences between blood levels of ^{201}Tl , [^{14}C]2DG and ^{99m}Tc -sestamibi grouped by time were assessed by one-way ANOVA, and the Tukey-Kramer HSD test was used.
3. Imaging: A paired *t*-test was used to compare the average tumor counts per minute per pixel between the two image sets.

RESULTS

Blood Kinetics

The blood activity of ^{99m}Tc -sestamibi, ^{201}Tl and [^{14}C]2DG was followed from 5 to 60 min after injection in the c-neu OncoMouseTM (Fig. 1). These time-activity curves reveal the time interval during which the agents are available for tumor uptake. While the dose-corrected tumor activity of the compounds was not significantly different at 60 min, [^{14}C]2DG was significantly higher than ^{99m}Tc -sestamibi and ^{201}Tl at earlier times.

Tumor Histology

The mammary neoplasms displayed a variety of histological patterns that appeared to be related to tumor size and growth. Smaller neoplasms generally had a compact cellular pattern. In these instances, tumor cells were arranged in dense sheets. As the neoplasms became larger, they developed a cribriform pattern (Fig. 2A, B). This arrangement resulted from the orientation of cells into pseudoacini which in some instances contained secretory material, degenerative cells and/or red blood cells. The compact-cellular pattern was often prominent toward the expanding margins of a neoplasm irrespective of its size

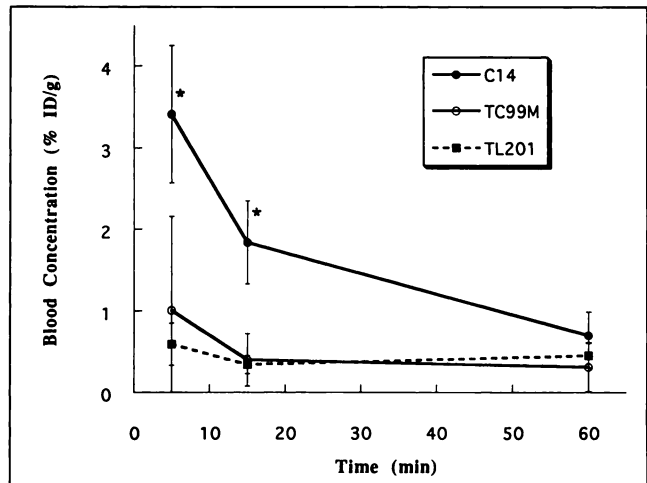


FIGURE 1. Blood activity after intravenous injection of 2 mCi ^{99m}Tc -sestamibi, 5 μCi [^{14}C]2DG and 0.3 mCi ^{201}Tl in the c-neu OncoMouseTM ($n = 3$), * $p < 0.05$ for ^{14}C versus ^{99m}Tc -sestamibi and ^{201}Tl .

(Fig. 2A). The presence of blood and/or degenerative tumor cells within these structures was usually evident in the centers of larger neoplasms.

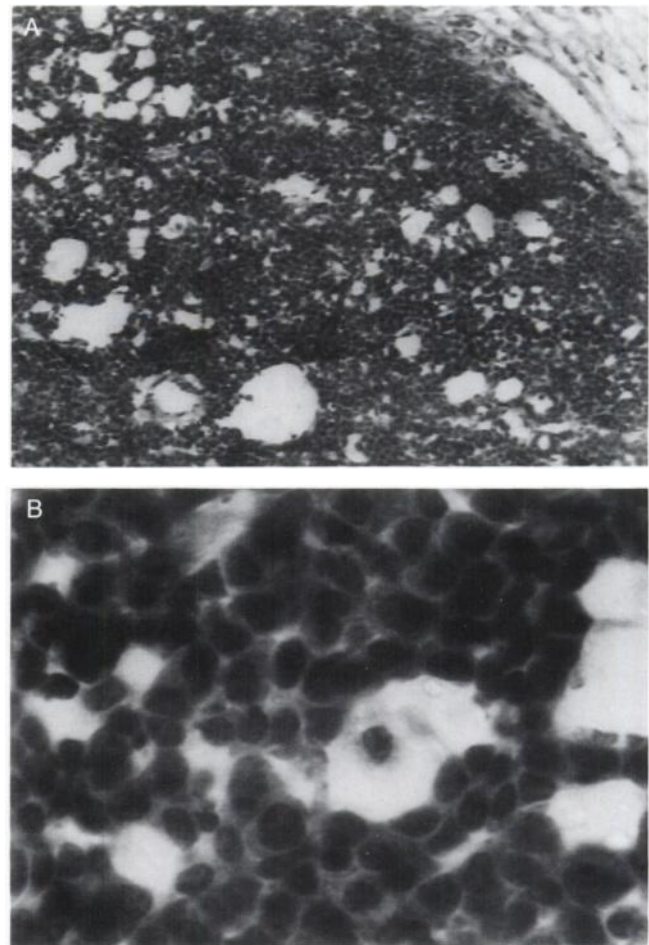


FIGURE 2. Cross-section through a mammary gland neoplasm in a c-neu OncoMouseTM. (A) Magnification $10\times$. and (B) $60\times$.

TABLE 1
Distribution of Technetium-99m-Sestamibi and Carbon-14-Deoxyglucose in the c-neu OncoMouse™*

Tissue	30 min p.i. (% ID/g)		60 min p.i. (% ID/g)	
	^{99m} Tc-sestamibi	[¹⁴ C]2DG	^{99m} Tc-sestamibi	[¹⁴ C]2DG
Tumor (peak)	0.94 ± 0.85	6.86 ± 1.33	0.95 ± 0.16	7.89 ± 2.30
Tumor (average)	0.38 ± 0.20	4.18 ± 0.62	0.52 ± 0.14	5.23 ± 0.89
Heart	2.18 ± 0.21	13.41 ± 4.27	2.27 ± 0.49	16.18 ± 5.70
Lung	0.29 ± 0.22	3.34 ± 1.00	0.30 ± 0.24	2.83 ± 0.70
Liver	2.71 ± 0.63	3.25 ± 0.29	2.32 ± 0.31	2.44 ± 1.70
Kidney	2.66 ± 0.68	4.56 ± 0.73	2.53 ± 0.53	3.84 ± 1.48
Muscle (femur)	1.00 ± 0.47	7.55 ± 2.35	0.58 ± 0.18	2.77 ± 1.27

*Data are the mean ± s.d. of three mice.

Small capillaries and larger blood vessels were always evident along the expanding margins of the neoplasm. The structures, however, were not easily delineated in the center of the neoplasms. With the exception of some degenerative neoplastic cells that were sloughed into the lumens of pseudoacini, areas of necrosis were not evident, even in the larger tumors. Neoplastic cells were moderately undifferentiated and contained large nuclei with scant amounts of neoplasm (Fig. 2B). The tumors appeared to grow by expansion. Evidence of invasion into surrounding tissue was not observed in any of the neoplasms nor were tumor emboli present in any discernable vascular or lymphatic spaces. Inflammation was not present in any of the neoplasms studied.

Distribution in Organs and Tumor

The biodistribution of ^{99m}Tc-sestamibi and [¹⁴C]2DG was examined in the c-neu OncoMouse™ using dual-label whole-body autoradiography. Thirty and 60 min postinjection were selected as experimental points to permit wash-out of free [¹⁴C]2DG from tissue and to overlap the period used in the imaging procedures. ROIs of organs and tumors were obtained from registered whole-body images of ¹⁴C and ^{99m}Tc activity, and the regions were assigned values of percent injected dose per gram tissue using standard microdensitometry.

The results of the dual-label study are summarized in Table 1. The activity of [¹⁴C]2DG was significantly higher than ^{99m}Tc-sestamibi in most organs, and [¹⁴C]2DG retention in the heart was particularly noteworthy (13–16% ID/g). The only significant change observed at 60 versus 30

min was a decrease in the retention of [¹⁴C]2DG in muscle ($p < 0.05$). The activity in the excretory organs was consistent with the known routes of elimination of the two agents, with high activity in the kidney for [¹⁴C]2DG, and high liver and gastrointestinal activity for ^{99m}Tc-sestamibi (gastrointestinal and bladder activity not shown).

The distribution of both ^{99m}Tc-sestamibi and [¹⁴C]2DG activity within the neoplasms was markedly heterogeneous (Fig. 3A, B) and tumor distribution is given as both average and peak activity in Table 1. The average tumor retention for [¹⁴C]2DG was ten times greater than for ^{99m}Tc-sestamibi. Peak tumor ^{99m}Tc-sestamibi activity was 0.94% ± 0.54% ID/g, with a range of 0.3%–1.9% ID/g. Inspection of the autoradiograms revealed a consistent pattern of intratumor retention for each of the two agents. Both [¹⁴C]2DG and ^{99m}Tc-sestamibi were retained in all tumors examined. Technetium-99m-sestamibi, however, had the highest activity at the periphery of the tumor, while peak [¹⁴C]2DG activity occurred at more interior regions.

A line segment image analysis of a set of registered ^{99m}Tc/¹⁴C tumor autoradiograms is displayed in Figure 4. In this procedure, a line of constant width and unit segment length is drawn as an ROI across the registered tumor images. The segment number on the x-axis is the unit distance from the periphery of the tumor, and the y-axis values are the amounts of radioactivity calculated within each line segment. With the outer periphery of the tumor at segment 1, ^{99m}Tc-sestamibi peaks near segment 5, while [¹⁴C]2DG is highest near segment 13. The peaking of [¹⁴C]2DG in interior regions relative to ^{99m}Tc-sestamibi

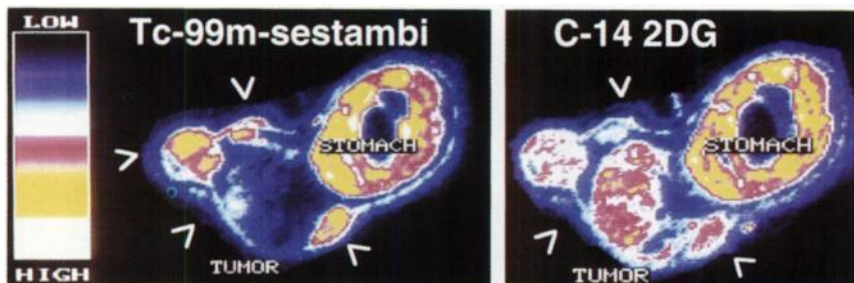


FIGURE 3. Technetium-99m (A) and ¹⁴C (B) autoradiographs of frozen whole-body sections from c-neu OncoMouse™ injected intravenously with 3 mCi ^{99m}Tc-sestamibi and 5 μCi [¹⁴C]2DG and euthanized 60 min postinjection.

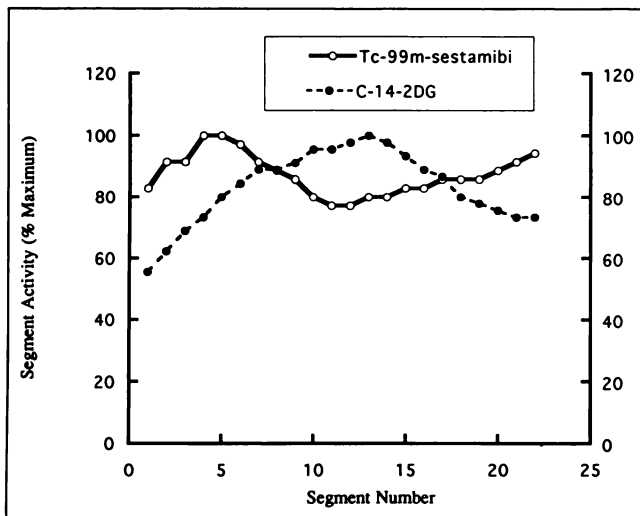


FIGURE 4. Line-segment analysis of intratumor activity of ^{99m}Tc -sestamibi and ^{14}C -2DG in a c-neu OncoMouse™. Segment 0 is the outer edge of the neoplasm and segment 22 is at the opposite edge.

was observed in all six animals. This shape of the segmented line pairs changed dramatically with each tumor, but the ^{14}C 2DG peak consistently occurred closer to the tumor center when compared to ^{99m}Tc -sestamibi.

Relationship of Agent Retention to Tumor Morphology

Autoradiograms of the neoplasms had a distinct patchy appearance. This was especially true for larger neoplasms. Comparison of the autoradiograms with the adjacent histological sections indicated that both radiolabeled agents were specifically being retained within the neoplastic cells, which grow in either the cribriform or compact cellular patterns: no retention occurred within the empty lumens of the pseudoacini. Thus, the patchy appearance of the autoradiograms resulted from a consistent restriction of the agents to the cellular portions of the neoplasms. In con-

FIGURE 5. Planar scintigraphy of ^{99m}Tc -sestamibi in a FVB (wild type) mouse.



trast, smaller tumors have a compact cellular histological form and a solid autoradiographic appearance.

The registered autoradiogram pairs of ^{99m}Tc -sestamibi and ^{14}C 2DG (Fig. 3) were also compared with adjacent 5-micron H&E-stained tissue sections. Tumor regions lacking histological evidence of cellular degeneration contained both ^{99m}Tc -sestamibi and ^{14}C 2DG activity. In contrast, neither agent had discernible activity present in lumens of pseudoacini or in areas of the neoplasms where evidence of cellular degeneration was prevalent. Regions adjacent to degenerative areas frequently had elevated ^{14}C 2DG activity and low ^{99m}Tc -sestamibi.

Planar Imaging

A protocol was developed for acquiring high-resolution planar images of mice. Wild type (FVB) mice ($n = 3$) were injected with ^{99m}Tc -sestamibi and imaged using this protocol background activity in the normal animal (Fig. 5). Since breast tumors arise spontaneously at any point within the mammary glands of the OncoMouse™, we attempted to

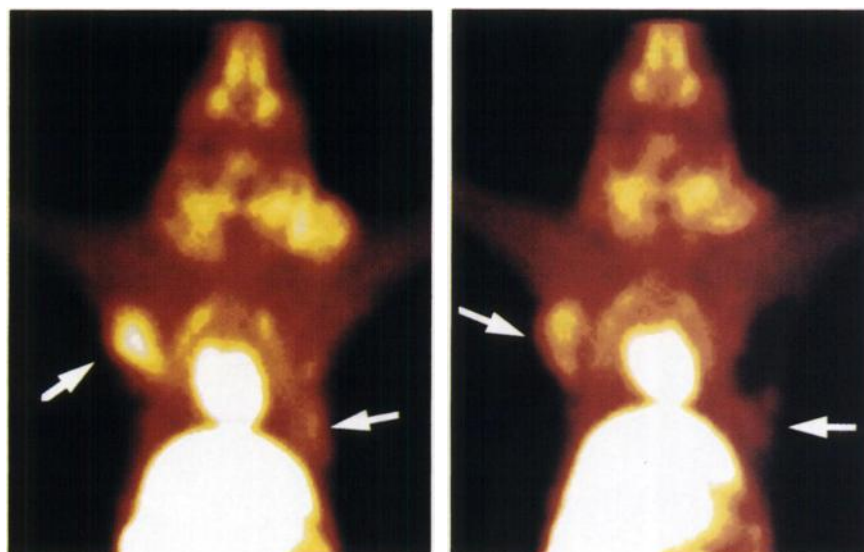


FIGURE 6. Planar scintigraphy of ^{99m}Tc -sestamibi in a c-neu OncoMouse™ (A). The mouse was reinjected 2 days later and re-imaged (B). A 1-cm lesion is visible to the left of the heart and one or more smaller lesions are present on the contralateral side.

ascertain which portions of the mammary epithelium could be imaged, free from significant interference from other organs. The image was windowed to allow visualization of the animal flank, where the mammary glands are located. As expected, pronounced activity was observed in the heart, liver and gut. In addition, large amounts of activity were present in the salivary glands, along with smaller regions near the nasal mucosa. The background activity along the animal's flank from below the neck to the top of the liver had uniformly low ^{99m}Tc -sestamibi uptake. Breast tumors arising within this region should therefore be easily distinguished from background activity.

Nine transgenic mice were imaged after ^{99m}Tc -sestamibi using a cross-over protocol. Each c-neu OncoMouse™ was imaged from 10 to 70 min after intravenous injection of 5–20 mCi ^{99m}Tc -sestamibi. Two to eight days later the mouse was reinjected with ^{99m}Tc -sestamibi and the imaging protocol was repeated. A typical image pair is displayed in Figure 6. This mouse is representative of most animals during the early stages of breast tumor growth. At later stages, several breast tumors would appear, many of which would become >1 cm in diameter with large radiodeficient centers. In Figure 6, a large tumor is evident in the subcutis to the left of the heart. On the opposite side, one or more smaller tumors are visible along the flank.

ROIs were drawn on the largest tumor from registered images of each of the nine image pairs. The average dose-corrected tumor activity was determined from these ROIs (561 ± 164 cpm/pixel, initial imaging, versus 559 ± 161 cpm/pixel, second imaging). No significant difference was observed between the image pairs ($p > 0.3$). The sensitivity of the method to detect differences (d) in tumor retention between a reference and test compound can be estimated from:

$$d = t * s/(n)^{-2},$$

where d = minimum detectable difference, t = value from the t distribution, s = s.d. and n = number of imaged pairs. For 9 pairs, $d = 2.306 * 163/(9)^{-2} = 125$ cpm/pixel. This represents a 22% detectable difference from the 560 mean. For a working preclinical screen with an n of 4 image pairs, $d = 173$ cpm/pixel and a detectable difference of 31%.

DISCUSSION

The ability to specifically localize within viable cells is an important criteria for a tumor imaging agent in distinguishing benign from malignant tissue. The retention of both ^{99m}Tc -sestamibi and [^{14}C]2DG in c-neu OncoMouse™ breast tumors was specifically restricted to histologically viable regions of the neoplasms. Fluorine-18-FDG has previously been used to image viable tissue in human breast tumors (1), and the present results indicate that ^{99m}Tc -sestamibi is likewise retained in viable breast tumor tissue. The cribriform or compact cellular histological appearance of the tumors also influenced the pattern of isotope distribution seen in the imaging studies. Whereas both agents

were retained in the compact cellular portions of the neoplasm, the lumens of the tumor cells were devoid of either isotope and arranged in pseudoacinar patterns. This finding suggests that histological patterns of tumor growth, as well as tissue viability, may significantly influence the appearance of a given tumor image. In this regard, it is important to note that a cribriform growth pattern is frequently observed in intraductal carcinomas of the human breast histologically (16).

Within viable areas of the neoplasm, significant heterogeneity of both [^{14}C]2DG and ^{99m}Tc -sestamibi distribution was observed. These distribution patterns were distinct and appeared to be related to the mechanism of retention of the agents. The tissue uptake and retention of [^{14}C]2DG is a multistep process, signifying the functionality of flow to the tumor, entry into the cell via the glucose transporter and phosphorylation by hexokinase. Carbon-14-2DG, a glucose analog, is avidly retained in glycolytic tissue, particularly in areas of hypoxia; and the oxygen content is known to fall rapidly within neoplasms (17). The distribution of [^{18}F]FDG in viable and necrotic myocardial tissue has been extensively investigated (18,19). Despite some reports of accumulation in necrotic tissue (20–22), [^{18}F]FDG is useful in marking viable tissue.

In the present study, the observed apex of [^{14}C]2DG tumor retention occurred in viable but presumably hypoxic interior regions. Technetium-99m-sestamibi retention, by contrast, is related to the negative potential on the mitochondrial membrane (10). Since the mitochondria require oxygen for maintenance of membrane potential, ^{99m}Tc -sestamibi retention should be predictably high in the well-perfused, normoxic periphery of the tumor, and should decrease with increased distance from blood vessels in the tumor interior. Thus the curves in Figure 4 may reflect the differential response of the two agents to contrasting patterns of oxygenation of the neoplasm.

The distribution and pharmacokinetic results indicate a much higher tumor retention (Table 1) and moderately prolonged blood level for [^{14}C]2DG (Fig. 1) compared to ^{99m}Tc -sestamibi and ^{201}Tl (Fig. 1). Prolonging circulating blood levels could contribute to higher tumor activity. The significantly higher tumor retention of [^{14}C]2DG observed in this study may translate to enhanced sensitivity for [^{18}F]FDG in human imaging with PET compared to ^{99m}Tc -sestamibi and ^{201}Tl . Whereas [^{18}F]FDG may have lower specificity due to uptake in macrophages (23,24), the absence of these cell types in the tumors could not be assessed in this model. The interior tumor regions, adjacent to areas of necrosis may contain hypoxic, pre-necrotic cells, in which [^{14}C]2DG is taken up by a nonmetabolic mechanism (25).

The [^{14}C]2DG tumor levels are significantly higher than those observed in transplanted rodent tumors (21), spontaneous dog tumors (20) and in rat brain tumors (26) and may vary directly with the magnitude of the tumor membrane potential (10). Other potential factors include variations in the animal model and assay technique. In addition,

the multidrug-resistant P-glycoprotein is potentially involved in the transport of ^{99m}Tc -sestamibi out of tumor cells (27). The decreased retention of ^{99m}Tc -sestamibi relative to [^{14}C]2DG in various tumor regions (Fig. 3A,B) may also be due to multidrug-resistant P-glycoprotein activity.

CONCLUSION

The c-neu OncoMouse™ is a useful model for in vivo imaging of breast tumors. We used a crossover protocol to assess ^{99m}Tc -sestamibi retention in a variety of spontaneous mammary tumors that have a blood supply and exhibit histological growth patterns closely approximating those found in ductal human breast carcinomas. The model has a predicted sensitivity to detect a 30% difference in tumor retention of a test versus reference compound in a preclinical screen. Technetium-99m-sestamibi was retained within mammary neoplasms in a pattern consistent with a viability marker. Technetium-99m-sestamibi tended to concentrate in more peripheral tumor regions than did [^{14}C]2DG. The c-neu OncoMouse™ provides a useful spontaneous tumor model for preclinical screening of breast tumor imaging agents.

ACKNOWLEDGMENTS

The authors thank Martin Thoolen, PhD and Walter Carney, PhD for helpful discussion, Michael Bresnick, MS for statistical analysis and Jim Toler and Mikhail Kagan for technical assistance.

REFERENCES

1. Wahl R, Cody R, Hutchins G, Mudgett E. Primary and metastatic breast carcinoma: initial clinical evaluation with PET with the radiolabeled glucose analog 2-[F-18]-fluoro-2-deoxy-D-glucose. *Radiology* 1991;179:765-770.
2. Tse N, Hoh C, Hawkins R. The application of PET imaging with fluorodeoxyglucose to the evaluation of breast disease. *Ann Surg* 1992;216:27-34.
3. Lamberts S, Krenning E, Reubi J. The role of somatostatin and its analogs in the diagnosis and treatment of tumors. *Endocrinol Rev* 1991;19:450-482.
4. Britten J, Blank M. Thallium activation of the (Na^+ , K^+) activated ATPase of rabbit kidney. *Biochim Biophys Acta* 1968;15:106-166.
5. Waxman A, Ramanna L, Memsic L, et al. Thallium scintigraphy in the evaluation of mass abnormalities of the breast. *J Nucl Med* 1993;34:18-23.
6. Lee VW, Sax EJ, McAneny DB, et al. A complementary role for thallium-201 scintigraphy with mammography in the diagnosis of breast cancer. *J Nucl Med* 1993;34:2095-2100.
7. Khalkhali I, Mena I, Diggles L. Review of imaging techniques for the diagnosis of breast cancer: a new role of prone scintimammography using technetium-99m-sestamibi. *Eur J Nucl Med* 1994;21:357-362.
8. Okada R, Glover D, Gaffney T, Williams S. Myocardial kinetics of technetium-99m-hexakis-2-methoxy-2-methylpropyl-isonitrile. *Circulation* 1988;77:491-498.
9. Crane P, Laliberté R, Heminway S, Thoolen M, Orlandi C. Effect of mitochondrial viability and metabolism on technetium-99m-sestamibi myocardial retention. *J Nucl Med* 1993;20:20-25.
10. Piwnica-Worms D, Kronauge J, Chiu M. Uptake and retention of hexakis-2-methoxyisobutylisonitrile technetium (I) in cultured chick cells: mitochondrial and plasma membrane potential dependence. *Circulation* 1990;82:1826-1838.
11. Shah S, Sands H. Preclinical models and methods for the study of radiolabeled monoclonal antibodies in cancer diagnosis and therapy. In: Goldenberg D, ed. *Cancer imaging with radiolabeled antibodies*. Norwell, MA: Kluwer; 1990:53-96.
12. Muller W, Sinn E, Pattengale P, Wallace R, Leder P. Single-step induction of mammary adenocarcinoma in transgenic mice bearing the activated c-neu oncogene. *Cell* 1988;51:105-115.
13. Pattengale P, Stewart T, Leder A, et al. Animal models of human disease. Pathology and molecular biology of spontaneous neoplasms occurring in transgenic mice carrying and expressing cellular oncogenesis. *Am J Pathology* 1989;135:39-61.
14. Lear J. Principles of single and multiple radionuclide autoradiography. In: Phelps M, Mazziotta J, Schelbert H, eds. *Positron emission tomography and autoradiography: principles and applications for the brain and heart*. New York: Raven Press; 1986:197-235.
15. Ito T, Brill B. Validity of tissue paste standards for quantitative whole-body autoradiography using short-lived radionuclides. *Appl Radio Isot* 1990;41:661-667.
16. Cotran RS, Kumar V, Robbins SL, Shoen F, eds. *Pathologic basis of disease*, 4th ed. Philadelphia: W.B. Saunders Co., 1994.
17. Vaupel P, Kallinowski F, Okunieff P. Blood flow, oxygen and nutrient supply, and metabolic environment of human tumors: a review. *Cancer Res* 1989;49:6449-6465.
18. Schelbert H. Metabolic imaging to assess myocardial viability. *J Nucl Med* 1994;35(suppl):8S-14S.
19. Bergmann S. Use and limitations of metabolic tracers labeled with positron-emitting radionuclides in the identification of viable myocardium. *J Nucl Med* 1994;35(suppl):15S-22S.
20. Larson SM, Weiden PL, Grunbaum Z, et al. Positron imaging feasibility studies. II: characteristics of 2-deoxyglucose uptake in rodent and canine neoplasms: concise communication. *J Nucl Med* 1981;22:875-879.
21. Som P, Atkins HL, Bandyopadhyay D, et al. A fluorinated glucose analog, 2-fluoro-2-deoxy-D-glucose (F-18): Nontoxic tracer for rapid tumor detection. *J Nucl Med* 1980;21:670-675.
22. Paul R, Johansson R, Kellokumpu-Lehtinen P, Söderström K, Kangas L. Tumor localization with 18F-2-fluoro-2-deoxy-D-glucose: comparative autoradiography, glucose 6-phosphatase histochemistry, and histology of renally implanted sarcomas of the rat. *Res Exp Med* 1985;185:87-94.
23. Kubota R, Yamada S, Kubota K, Ishiwata K, Tamahashi N, Ido T. Intratumoral distribution of fluorine-18-fluorodeoxyglucose in vivo: high accumulation in macrophages and granulation tissues studied by microautoradiography. *J Nucl Med* 1992;33:1972-1980.
24. Hoh C, Hawkins R, Glaspy J, et al. Cancer detection with whole-body PET using 2-[^{18}F]fluoro-2-deoxy-D-glucose. *J Comput Assist Tomogr* 1993;17:582-589.
25. Kubota R, Kubota K, Yamada S, Tada M, Ido T, Tamahashi N. Active and passive mechanisms of [Fluorine-18] fluorodeoxyglucose uptake by proliferating and preneoplastic cancer cells in vivo: a microautoradiographic study. *J Nucl Med* 1994;35:1067-1075.
26. Packard AB, Kronauge JF, Limpa-Amara N, Lampson L, O'Tuama L, Jones AG. Tumor uptake of ^{99m}Tc -MIBI and ^{201}Tl by a 9L gliosarcoma brain tumor model in rats. *Nuc Med Biol* 1993;20(6):773-776.
27. Piwnica-Worms D, Chiu M, Budding M, Kronauge J, Kramer R, Croop J. Functional imaging of multidrug-resistant P-glycoprotein with an organo-technetium complex. *Cancer Res* 1993;53:977-984.